Effects of resonances on halo formation in high-intensity storage rings

D. Jeon, J. A. Holmes, V. V. Danilov, J. D. Galambos, and D. K. Olsen
SNS Bldg MS-8218, Oak Ridge National Laboratory, 104 Union Valley Road, Oak Ridge, Tennessee 37831
(Received 4 February 1999; revised manuscript received 2 September 1999)

Numerical calculations for the Spallation Neutron Source accumulator ring indicate that lattice resonances excited by the space-charge potential can increase a mismatch significantly by deforming the beam distribution in phase space. Hence increased mismatch leads to enhanced envelope oscillations that are driving the 2:1 parametric resonance leading to halo formation, even for initially matched beams. We have observed this behavior for the $2\nu_x-2\nu_y=0$ resonance and for the $4\nu_y=23$ resonance. This mechanism for halo formation peculiar to rings through resonance driven mismatch is very sensitive to the tunes, which emphasizes the importance of a careful choice of operating point in tune space. [S1063-651X(99)10012-6]

PACS number(s): 29.27.Bd

I. INTRODUCTION

The acceleration of intense beams has become very relevant due to a number of important applications. These include neutron scattering, the transmutation of nuclear waste, tritium production, and accelerator-driven fusion. For example, the accelerator system of the Spallation Neutron Source (SNS) [1] will deliver a 1 GeV pulsed proton beam to a liquid Hg target at 60 Hz. The accumulator ring is being designed to support 2 MW of beam, which implies that it must be capable of storing more than 2×10^{14} protons in each pulse. In order to expedite hands-on maintenance, there are stringent requirements for uncontrolled losses, namely about one part in 10^6 per meter. Because of this combination of high beam intensity and low uncontrolled loss requirements, space-charge contributions to beam loss and halo formation are of crucial importance to the SNS and other high-intensity projects.

Space-charge effects have been studied for many years, particularly for linear accelerators. Kapchinskij and Vladimirskij derived an envelope equation and an analytic self-consistent equilibrium distribution function, called the KV distribution [2]. Since this pioneering work, much progress has been made through the development and generalization of such concepts as rms emittance, the envelope equation, etc. [3–5]. Numerical simulations, mostly for linacs, and the particle core model indicate that the principal cause of space-charge-induced halo is the 2:1 parametric resonance excited by the envelope oscillations of mismatched beams [3–9]. The extension of this work to detailed numerical calculations of space-charge dynamics in rings is the subject of this paper. In particular, we show that lattice resonances both excite the 2:1 parametric resonance and enhance the access of beam particles to this halo-forming resonance. This previously unknown two-step resonance mechanism can form appreciable halos in rings even for a very small tune depression of about 1%, unlike tens of percents of tune depression usually considered in linacs.

The study is carried out using the lattice and beam parameters of the 2 MW SNS accumulator ring where a 1 GeV H^- beam from the linac is injected into a dispersion-free straight section. The ring is fourfold symmetric consisting of 24 FODO cells and having a 221 m circumference. The nominal bare tunes are $\nu_x=5.82$ and $\nu_y=5.80$. The tune depression due to space-charge effects is $\Delta\nu\approx0.08$, or about 1.4%. In this study, no injection process is simulated. We tracked beams for many turns starting from the initial distribution of 2 MW beam at 0 turn.

The ACCSIM code with two-dimensional particle-in-cell (2D-PIC) space-charge evaluation is used [10]. We treat the beam dynamics in transverse phase space assuming a coasting beam with energy spread ±9.4 MeV. The ACCSIM code treats the lattice using linear transfer matrices generated by the DIMAD code. Any higher-order multipoles are not included, in numerical simulations. Also any skew lattice elements are not included such as skew quadrupoles. Consequently, the space-charge potential provides the only nonlinearities in the Hamiltonian and it is easy to identify the specific effects of the space-charge potential. The calculations presented here utilize numerically generated KV-like distributions with energy spread for the initial beam distributions. To examine the effects of lattice resonances here, we carry out all calculations with horizontal bare tune $\nu_x=5.82$ and vary the vertical bare tune from case to case.

Even though difference resonances are not usually regarded as dangerous to the operation of accelerators because of the conservation of J_x+J_y, where $J_{x(y)}$ is the $x(y)$ action, we show in Sec. II that the Montague resonance $2\nu_x-2\nu_y=0$ can become excited due to space charge and enhance halo formation dramatically in rings with intense beam. Furthermore, in Sec. III, we show that the fourth-order resonance $4\nu_y=23$ from space charge also induces a mismatch by deforming beam distributions in phase space that leads to significant halo formation for an initially well-matched beam. In both of these cases, the lattice resonances are driven by even-mode space-charge potentials. In Sec. IV, conclusions from this work are summarized.

II. EFFECTS OF DIFFERENCE RESONANCES

Hofmann [11] showed, using self-consistent Vlasov-Poisson equations, that the space-charge potential can support an even-mode space-charge potential,

$$\Phi_{4,e}=a_0x^4+a_2x^2y^2+a_4y^4, \tag{2.1}$$

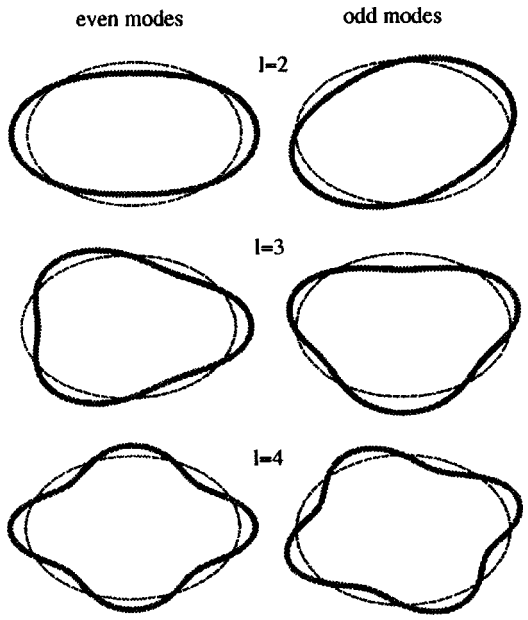

FIG. 1. Beam cross sections for even and odd modes up to the fourth order. This figure and terminology are borrowed from Dr. Ingo Hofmann with his permission.

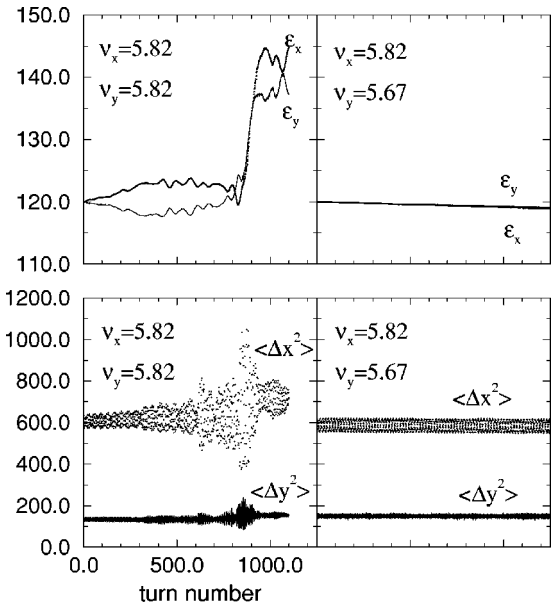

FIG. 2. Plots of rms emittances (top plots) in π mmmrad and the second moments $\langle \Delta x^2 \rangle$ and $\langle \Delta y^2 \rangle$ (bottom plots) in mm^2 for two cases. The tunes in the plots are bare tunes. Initially 3% mismatched beams are used for both cases. When the tunes are equal, strong-coupling effects are induced leading to a rms emittance growth at about 900 turns.

inside the beam. Figure 1 is a schematic drawing of the beam cross sections of even- and odd-mode space-charge potentials up to the fourth-order. The fourth order coupling term, shown in Eq. (2.1), can excite the difference resonance $2\nu_x - 2\nu_y = n$ with integer n. We examine now the effect of exciting this Montague resonance, in which $n=0$. To do this we consider two cases with vertical bare tunes $\nu_y = 5.82$ and $\nu_y = 5.67$, respectively. In the first case, the tune separation is 0 and we anticipate strong excitation of the difference resonance, while in the second case the tune separation is 0.15 and the excitation should be less. In both cases the initial beams are given a radial mismatch of 3%, which is quite small compared with the mismatch considered in linacs to observe halo formation (generally a few tens of percent). 20 000 macroparticles are used for numerical simulations except for a few cases where more resolution in phase-space distributions is required. In this case, 100 000 macroparticles are used. Simulations by varying the number of macroparticles show that 20 000 macroparticles are quite enough.

Figure 2 shows the rms emittances and the second moments $\langle \Delta x^2 \rangle$ and $\langle \Delta y^2 \rangle$ in mm^2 for the two cases. The oscillation amplitude of the second moments is a measure of beam envelope oscillations. When the tunes are equal, a sudden and massive emittance growth is induced simultaneously in both planes at about 900 turns. This is preceded by a rapid growth in the oscillation amplitudes of $\langle \Delta x^2 \rangle$ and $\langle \Delta y^2 \rangle$ at about 850 turns. Following the emittance growth, the oscillations of the second moments subside, reflecting the existence of a new relaxed beam equilibrium with halo. In contrast, in the case having unequal tunes the beam is fairly stable, with little emittance growth, even though the beam has the same initial mismatch as the case of $\nu_x = 5.82$ and $\nu_y = 5.82$.

Figure 3 shows that the $\langle \Delta x^2 \Delta y^2 \rangle$ moment in mm^4, for the case $\nu_x = 5.82$ and $\nu_y = 5.82$, increases dramatically reaching peak at around 850 turns prior to the sudden emittance growth at around 900 turns, much the same as the second moments. This particular moment reflects the coupling term in Eq. (2.1) that can excite $2\nu_x - 2\nu_y = 0$ resonance, and its behavior supports the involvement of this resonance in the emittance growth in the case having equal tunes. During the emittance blow-up, asymmetry in the particle distribution is also induced generating weak odd-mode space-charge potentials. Figure 3 shows that a sudden growth of the asymmetric $\langle \Delta x \Delta y \rangle$ moment is induced at about 900 turns when the emittance growth takes place. This shows an inducement of small asymmetry in the particle distribution that can induce the second-order odd-mode potential $\Phi_{2,o} = a_1 xy$ [11]. This potential can excite the $\nu_x - \nu_y = n$ resonance. However, it should be noted that the maximum oscillation amplitude of $\langle \Delta x^2 \Delta y^2 \rangle$ moment is at about 850 turns while that of $\langle \Delta x \Delta y \rangle$ moment occurs at about 940 turns. It is

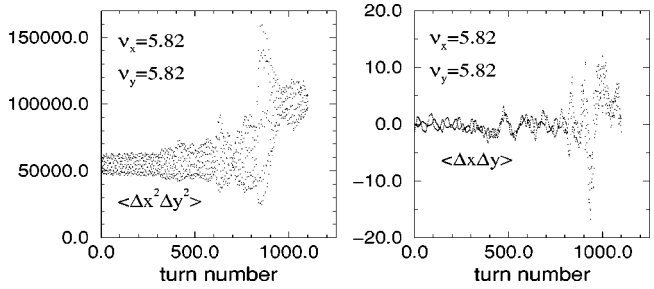

FIG. 3. Plots of the fourth moment $\langle \Delta x^2 \Delta y^2 \rangle$ in mm^4 and the second moment $\langle \Delta x \Delta y \rangle$ in mm^2 for the beam in Fig. 2. Before the sudden emittance growth at about 900 turns (top left plot of Fig. 2), the $\langle \Delta x^2 \Delta y^2 \rangle$ moment that excites the $2\nu_x - 2\nu_y = 0$ resonance grows dramatically, reaching peak at about 850 turns. When the sudden emittance growth takes place, asymmetric second moment $\langle \Delta x \Delta y \rangle$ is also induced (reaching maximum at about 940 turns) that can excite the $\nu_x - \nu_y = 0$ resonance.

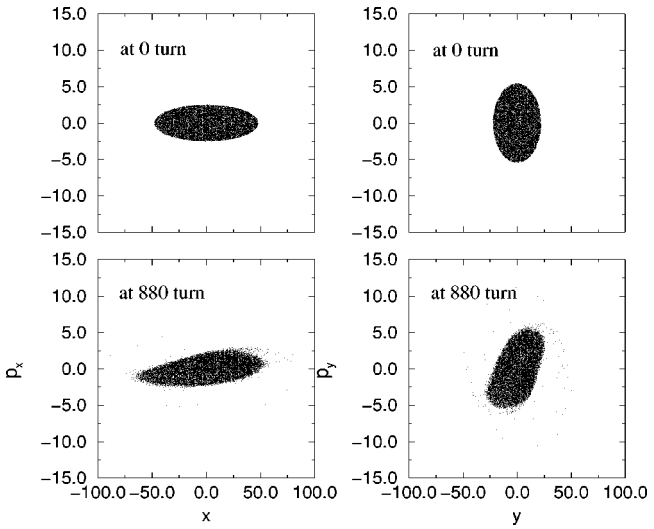

FIG. 4. Plots of the beam particle distributions in both phase spaces. The top plots are the initial KV-like particle distributions. The bottom plots show the deformation in the particle distributions at 880 turns due to the difference resonance. This deformation makes the beam more mismatched. x and y are in mm, and p_x and p_y in mrad.

clear that changes in the $\langle \Delta x^2 \Delta y^2 \rangle$ moment are leading the entire process. Besides, even-mode particle distributions which are symmetric with respect to the midplane are strongly favored as equilibrium particle distributions rather than odd-mode potentials due to the midplane symmetry of the accelerator. So the dominant lattice resonance responsible for the emittance blow-up is the $2\nu_x - 2\nu_y = 0$ resonance rather than the $\nu_x - \nu_y = 0$ resonance.

Figure 4 shows the induced deformation in the particle distribution due to the difference resonance at 880 turns in both phase spaces. The width of the beam has grown in both dimensions x and y, and the envelope is severely deformed. The point is that the beam distribution changes as time goes on due to the the lattice resonance $2\nu_x - 2\nu_y = 0$. This deformation of the beam distributions induces an even larger mismatch and envelope oscillations evidenced clearly by the dramatic increase in the oscillation amplitude of second moments shown in the left lower plot of Fig. 2. On the contrary, nothing happens for $\nu_x = 5.82$ and $\nu_y = 5.67$ being far from the lattice difference resonance.

Numerical simulations indicate that the width of the Montague resonance is $|\nu_x - \nu_y| < 0.04$. The Montague resonance, $2\nu_x - 2\nu_y = 0$, facilitates halo generation in two ways: (i) by increasing the strength of the 2:1 parametric resonance through the coupling of the horizontal and vertical envelope oscillations; and (ii) by helping particles, through the coupling, to jump across the separatrices of the 2:1 parametric resonance. The increased oscillation amplitude of the second moments for the case of equal tunes shows the enhancement of the envelope oscillations of the beam by the coupling resonance. The increased strength of the 2:1 parametric resonance is also demonstrated by the large extent of the separatrix and halo in Fig. 5 that shows the corresponding particle distributions in phase space for both cases at 1100 turns. In general, we expect the strength of the $2\nu_x - 2\nu_y = nP$ resonance to be significant when P is the superperiod of a lattice and n is an integer.

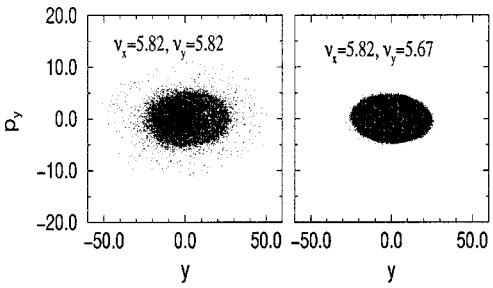

FIG. 5. Plots of the beam particle distributions in phase space for the two cases in Fig. 2 at 1100 turns. In the case having equal tunes, a significant halo is generated in contrast to the other case. Also, a denser region in the particle distribution has developed, shown in the left part of the core in the left plot. 20 000 macroparticles are used for the simulation. y is in mm and p_y in mrad.

Figure 6 shows the case of a well-matched beam (radially with less than 1% mismatch) having $\nu_x = 5.82$ and $\nu_y = 5.82$. The small initial oscillations in the second moments are due to the tiny initial mismatch (compare this amplitude with that in Fig. 2). The difference resonance is excited by the nonuniformities in the numerical distribution and this leads to a further mismatch, as shown by the increasing oscillation amplitudes of $\langle \Delta x^2 \rangle$. Even in the case of a well-matched beam, when the tunes are equal the Montague resonance, $2\nu_x - 2\nu_y = 0$, will be excited, and will ultimately strongly excite strong envelope oscillations indicated by the huge oscillation amplitude of second moments at around 2300 turns. This well-matched case is observed to remain stable for over 2000 turns, but ultimately the emittance increases dramatically, driven by the mismatch caused by the difference resonance $2\nu_x - 2\nu_y = 0$.

Numerical calculations using bare tunes of $\nu_x = 5.82$ and $\nu_y = 4.82$ indicate that the effects of the $2\nu_x - 2\nu_y = 2$ resonance are negligible. This is an imperfection resonance in the fourfold symmetric SNS accumulator ring. It is obvious that the driving of this particular resonance by the space-charge potential is negligible. Nonetheless, caution should be taken regarding such configurations in accelerator design because skew components also arise from lattice imperfections. While it is also necessary to study the effects of the higher-order difference resonances $l\nu_x - m\nu_y = n$, where l, m, and n are integers, we do not pursue that subject here.

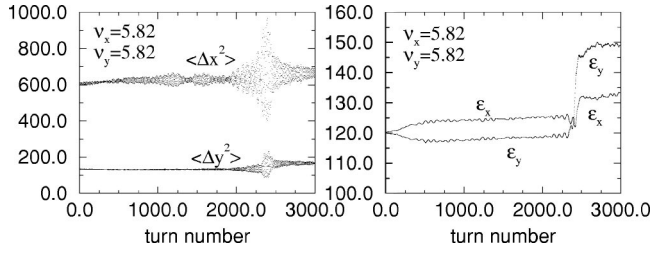

FIG. 6. Plots of the second moments $\langle \Delta x^2 \rangle$ and $\langle \Delta y^2 \rangle$ (left plot) in mm^2 and the emittances (right plot) in π mmmrad for a well-matched beam with an initial mismatch less than 1%. The tunes are bare tunes. Increasing oscillation amplitudes of $\langle \Delta x^2 \rangle$ are observed. At around 1900 turns, strong coupling effects are induced leading to a significant emittance growth and an equilibrium.

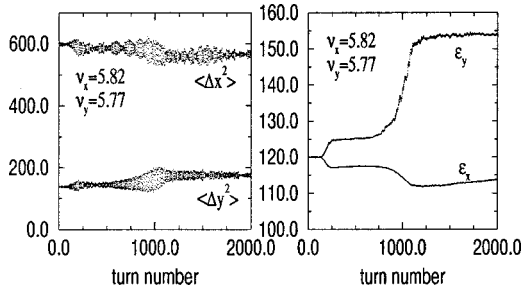

FIG. 7. Plots of the second moments $\langle \Delta x^2 \rangle$ and $\langle \Delta y^2 \rangle$ (left plot) in mm^2 and the emittances (right plot) in π mmmrad for a well-matched beam. The first y emittance growth is due to the $4\nu_y = 23$ resonance and the second growth due to the mismatch thus generated.

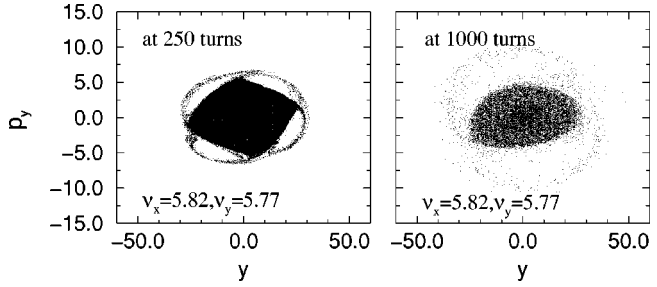

FIG. 8. Plots of the particle distribution in y phase space at 250 turns and at 1000 turns for the beam in Fig. 7. The structure of the fourth-order resonance $4\nu_y = 23$ is clearly shown in the left plot, where 100 000 macroparticles are used for better resolution. The right plot evidently shows the 2:1 parametric resonance, driven by the mismatch generated by the $4\nu_y = 23$ resonance, where 20 000 macroparticles are used. y is in mm and p_y in mrad.

III. EFFECTS OF OTHER RESONANCES

Odd-mode space-charge potentials are skew terms in the Hamiltonian and are small compared with even modes in lattices with midplane symmetry. Consequently, the resonances of these odd modes are weak. However, even-mode space-charge potentials are not weak, and are consequently easy to observe. For example, the $4\nu_y = n$ resonance [12], shown in Fig. 8, which is associated with the fourth-order even-mode potential $\Phi_{4,e} = a_0 x^4 + a_2 x^2 y^2 + a_4 y^4$ [11], is stronger than the $3\nu_y = n$ resonance associated with the third-order odd-mode potential $\Phi_{3,o} = a_1 x^2 y + a_3 y^3$ [11].

When the coherent tune is near a nonlinear resonance [13] associated with even-mode potentials, the excited resonance can generate a mismatch, even though the initial beam is well matched. Thus generated, the mismatch can drive the 2:1 parametric resonance and expedite halo formation. Figure 7 illustrates this process for a matched beam having bare tunes $\nu_x = 5.82$ and $\nu_y = 5.77$. The first moderate emittance increase is near 200 turns which is due to the excitation of the fourth-order $4\nu_y = 23$ resonance. The left plot in Fig. 8 is a snapshot of particle distributions in y phase space taken at 250 turns immediately after the first y emittance increase. It shows the structure of this resonance very clearly. With the beam thus mismatched, the second increase in the y emittance results from the excitation of the 2:1 parametric resonance. The right-hand plot in Fig. 8, of vertical phase space at 1000 turns, clearly shows the structure of the parametric resonance and the corresponding beam halo. The tune difference here is 0.05, so that the Montague resonance may also contribute to some extent.

It is advantageous to avoid nonlinear resonances associated with even-mode space-charge potentials when choosing an operating point for intense beam circular accelerators. This is especially true when the horizontal and vertical tunes are close.

IV. CONCLUSIONS

Numerical simulations indicate that a strong mismatch can be induced through the deformation of the beam distribution in phase space by lattice resonances excited by the space-charge potential, even for an initially well-matched beam. This mismatch can then lead to significant halo generation, even for the quite weak tune depressions of 1–2 % typical of high intensity rings. This two-stage process for halo generation is peculiar to the rings, and is initiated by a fundamentally different mechanism from that in linear accelerators.

This mechanism for halo generation is of considerable interest by itself, but its crucial impact is that it can lead to a better design to minimize beam-loss halos in high-intensity rings. All of the dynamics studied in this work are very sensitive to the choice of operating point in tune space. A detailed study of halo generation in tune space will be required to find an operating point that minimizes halos.

ACKNOWLEDGMENTS

This work was supported by the Division of Materials Science, U.S. DOE, under Contract No. DE-AC05-96OR22464 with Lockheed Martin Energy Research Corporation for Oak Ridge National Laboratory.

[1] National Spallation Neutron Source Conceptual Design Report, Volumes 1 and 2, NSNS/CDR-2/V1,2 (May, 1997); on the World Wide Web at http://www.ornl.gov/ nsns/ CDRDocuments/CDR.html

[2] I.M. Kapchinskij and V.V. Vladimirskij, *Proceedings of the 9th International Conference on High Energy Accelerators*, edited by L. Kowarski (CERN, Geneva, 1959), p. 274.

[3] P.M. Lapostolle, IEEE Trans. Nucl. Sci. **NS-18**, 1101 (1971); F.J. Sacherer, *ibid.* **NS-18**, 1105 (1971); J.D. Lawson, P.M. Lapostolle, and R.L. Gluckstern, Part. Accel. **5**, 61 (1973); E.P. Lee and R.K. Cooper, *ibid.* **7**, 83 (1976).

[4] C. Chen and R.C. Davidson, Phys. Rev. E **49**, 5679 (1994); Phys. Rev. Lett. **72**, 2195 (1994).

[5] S.Y. Lee and A. Riabko, Phys. Rev. E **51**, 1609 (1995); A. Riabko *et al.*, *ibid.* **51**, 3529 (1995).

[6] R.A. Jameson, *Proceedings of the 1993 Particle Accelerator Conference* (IEEE, Piscataway, NJ, 1993), p. 3926.

[7] J.S. O'Connell, T.P. Wangler, R.S. Mills, and K.R. Crandall, *Proceedings of the 1993 Particle Accelerator Conference* (IEEE, Piscataway, NJ, 1993), p. 3657.

[8] J.M. Lagniel, Nucl. Instrum. Methods Phys. Res. A **345**, 46 (1994); **345**, 405 (1994).

[9] I. Hofmann, L.J. Laslett, L. Smith, and I. Haber, Part. Accel. **13**, 145 (1983); J. Struckmeier and M. Reiser, *ibid.* **14**, 227 (1983).

[10] J.A. Holmes *et al.* (unpublished); F. Jones, Users' Guide to ACCSIM, TRIUMF Design Note, TRI-DN-90-17 (1990).

[11] I. Hofmann, Phys. Rev. E **57**, 4713 (1998).

[12] S. Machida and Y. Shoji, in *Space Charge Dominated Beams and Applications of High Brightness Beams*, edited by S.Y. Lee, AIP Conf. Proc. No 377 (AIP, New York, 1996), p. 160.

[13] R. Baartman, *Workshop on Space Charge Physics in High Intensity Hadron Rings*, edited by A.U. Luccio and W. Weng, AIP Conf. Proc. No. 448 (AIP, New York, 1996), p. 56.